

# GmNet: Revisiting Gating Mechanisms From A Frequency View

Yifan Wang<sup>1</sup> Xu Ma<sup>1</sup> Yitian Zhang<sup>1</sup> Zhongruo Wang<sup>2</sup>  
 Sung-Cheol Kim<sup>3</sup> Vahid Mirjalili<sup>3</sup> Vidya Renganathan<sup>3</sup> Yun Fu<sup>1</sup>  
<sup>1</sup> Northeastern University <sup>2</sup> UC Davis <sup>3</sup> FM-Global  
 {wang.yifan25, ma.xu1, zhang.yitian}@northeastern.edu, wangleft@gmail.com,  
 {sungcheol.kim, Vahid.Mirjalili, Vidya.Renganathan}@fmglobal.com, yunfu@ece.neu.edu

## Abstract

Gating mechanisms have emerged as an effective strategy integrated into model designs beyond recurrent neural networks for addressing long-range dependency problems. In a broad understanding, it provides adaptive control over the information flow while maintaining computational efficiency. However, there is a lack of theoretical analysis on how the gating mechanism works in neural networks. In this paper, inspired by the convolution theorem, we systematically explore the effect of gating mechanisms on the training dynamics of neural networks from a frequency perspective. We investigate the interact between the element-wise product and activation functions in managing the responses to different frequency components. Leveraging these insights, we propose a Gating Mechanism Network (GmNet), a lightweight model designed to efficiently utilize the information of various frequency components. It minimizes the low-frequency bias present in existing lightweight models. GmNet achieves impressive performance in terms of both effectiveness and efficiency in the image classification task. Our code is public at <https://github.com/YFWang1999/GmNet>

## 1. Introduction

The gating mechanism has been widely used in recurrent neural networks (RNNs) [3, 13] to address long-term dependency issues. With the flourish of Transformers [29], self-attention-based architectures have largely replaced RNNs as the core model in natural language processing (NLP). Despite their success, scaling Transformers to long sequences remains challenging due to the quadratic complexity of global attention. Linear gating mechanisms (*i.e.* Gated Linear Units [4]) have been rediscovered as an effective approach to address this problem.

Gated Linear Units (GLUs) introduce a gating mechanism that adaptively controls information flow, allowing the model to focus on relevant features and ignore less impor-

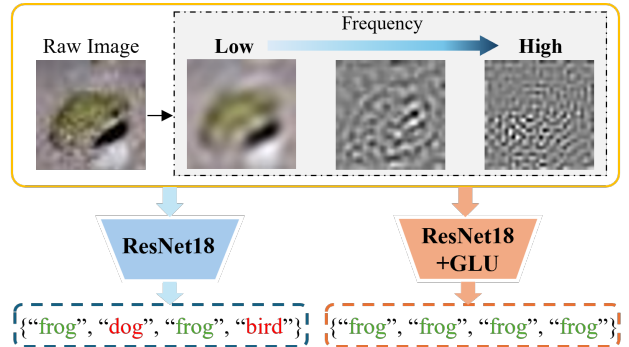


Figure 1. An illustration of how GLUs affect neural networks in classifying different frequency parts of an image. Starting with a raw image of a frog, we break it down into different frequency bands. The lowest frequency shows a recognizable outline, the middle frequency retains the general shape of the frog, but the highest frequency is almost unrecognizable. Predictions of different components are given in the lower of different models.

tant ones. These architectures are simple to implement, and have no apparent computational drawbacks. Therefore, models built with GLUs have been developed in various tasks across NLP [5, 6, 10] and Computer Vision [16, 18, 33]. While architectures based on linear gating mechanisms have demonstrated the effectiveness, their theoretical analysis have not received enough attention. Except intuitive explanations, a deeper examination of their mathematical properties could provide valuable insights for the development of efficient gating mechanisms. Inspired by the Fourier interpretation of element-wise product, we propose to investigate training dynamics of neural networks (NNs) with gating mechanisms from a frequency perspective. This approach helps us understand how frequency components are selectively amplified or suppressed during learning. By the frequency analysis, we aim to uncover how GLUs influence the spectral properties of neural networks and affect the overall performance.

To begin with, we present an intuitive example that il-

illustrates the responses of neural networks to different frequency components of an image. The example as shown in Fig. 1 demonstrates two key points. First, NNs can utilize specific frequency components for classification, not just the low-frequency ones as commonly assumed. This indicates that high-frequency information can also be critical for accurate classification tasks. Second, Gated Linear Units can enhance NNs’ ability of effectively learning and integrating different frequency components.

In this paper, we systematically explore how gating mechanisms impact the training dynamics. We also provide a comprehensive understanding of how the element-wise product and activation functions interplay to shape the frequency response of neural networks. The first observation is inspired by the *convolution theorem* and convolution operation in the frequency domain. It indicates that element-wise multiplication in the spatial domain, equivalent to convolution in the frequency domain, inherently introduces new frequency components. It may enhance the learned representations for various frequency domains. However, as demonstrated in prior studies [31, 34], NNs are sensitive to high-frequency noise, which may adversely influence training stability and generalization. Therefore, it is necessary to include activation functions within the gating units to regulate the newly introduced frequency components. Activation functions can broadly be classified based on their differential properties. Smooth activation functions (GELU [12] and Swish), characterized by continuous higher-order derivatives, tend to introduce fewer high-frequency components. On the other hand, activation functions (ReLU) with discontinuous higher-order derivatives are more likely to encourage the learning of high-frequency components.

Benefited by the sufficient study from the frequency view, we find that the existing lightweight methods are not aware of how to efficiently and effectively utilize the high-frequency information. In this paper, we incorporate the simplest gated linear unit into the current block design and come up with a competitive lightweight model named as **Gating Mechanism Network (GmNet)**. Our proposed network can more effectively capture information across different frequencies, offering both theoretical and practical advantages. With a simplified architecture of the network design, GmNet is able to achieve superior results compared with existing efficient modals without training with advanced techniques. For example, compared to EfficientFormer-L1 [14], GmNet-S3 outperforms 4.0% on top-1 accuracy on ImageNet-1K with 4x faster latency on an A100 GPU.

We succinctly summarize and emphasize the key contributions of this work as following points:

- We present a comprehensive study on how gated linear units influence neural network training dynamics from a frequency perspective. Through both theoretical analy-

sis and experimental evidences, we demonstrate how the interaction between element-wise multiplication and activation functions shapes the frequency response of NNs.

- Inspired by the study of the gating mechanism, we proposed a competitive lightweight model, named **Gating Mechanism Network (GmNet)**, which achieves promising performance without the need for strong training strategy, surpassing numerous efficient designs.

## 2. Related Work

**Gated Linear Units.** Gating mechanisms have been extensively utilized in neural networks for sequence data processing tasks [4, 7, 9, 13]. With the rise of Transformer architectures, the Gated Linear Unit [24] has been revisited and recognized as an efficient and effective enhancement for modern deep learning models. Recent research has increasingly focused on the integration of gating mechanisms into diverse network architectures of different tasks, including gate-MLP [16], Mamba [10] and Llama3 [6]. While many existing studies provide high-level insights into the functional role of gating mechanisms, there is a notable lack of in-depth analysis of their underlying learning processes. In this work, we conduct a series of experiments combined with solid theoretical analysis to elucidate the roles of gating mechanisms in enhancing the learning of neural networks. Specifically, we investigate the types of information that gating encourages networks to capture from a frequency perspective.

**Frequency Learning.** Understanding the learning dynamics of neural networks from a frequency perspective is an increasingly interesting topic. It has been found that neural networks respond differently to frequency information depending on the tasks. It has been investigated that neural networks tend to learn low-frequency components quickly before fitting the high-frequency ones for regression tasks [22, 25, 34]. In classification tasks, by investigating how neural networks respond to different frequency components during training, researchers found that there exists a trade-off between the accuracy and robustness [31]. NNs can improve the accuracy by learning more from high frequency components but they are also sensitive to high frequency noise which may disturb the training of NNs. In this paper, we investigate how GLUs optimize the trade-off which drive us to propose a new efficient model design.

**Lightweight Networks.** The existing lightweight networks can be categorized into two types: (1) Pure convolution-based networks like MobileOne [28], StarNet[18] and RepVit[30]; (2) Self-attention-based architectures including EfficientMod[19] and EfficientFormerV2[14]. Although existing network designs already achieve promising performance, they still exhibit significant shortcomings from the

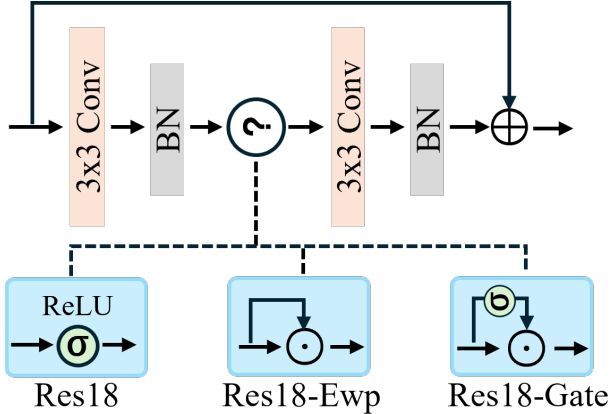


Figure 2. Block design of different variants of ResNet18 where  $\odot$  represents the element-wise product and  $\sigma$  means the activation function. In this paper, we primarily investigate GLUs using ReLU and GELU as activation functions where corresponding variants can be named as Res18-Gate-ReLU or Res18-Gate-GELU.

perspective of the frequency view. Both convolution and self-attention are learning methods with a low-frequency bias [1, 26]. Furthermore, because compact networks typically focus on minimizing parameters and simplifying model structure, their capacity to capture high-frequency details may be restricted. In this paper, we propose a new competitive and efficient network that demonstrates the effectiveness of learning from higher frequency components.

### 3. Revisiting Gating Mechanisms from A Frequency View

To better understand how gating mechanisms work, this paper investigates the behavior of a convolutional neural network (CNN) in classification tasks from a frequency perspective. We begin by defining the components associated with different frequency bands and outlining the details of our experimental setup.

With decomposing the raw data into a series data  $\mathbf{z} = \{\mathbf{z}_i\}_{i=0}^n$ ,  $\mathbf{z}_i$  represent different frequency components of an image  $\mathbf{x}$ . Denoting a series thresholds  $R = [0, r_1, \dots, r_N, +\infty]$ , we have the following equations:

$$\mathbf{z} = \mathcal{F}(\mathbf{x}), \quad \mathbf{z}_0, \dots, \mathbf{z}_n = \theta(\mathbf{z}; R) \quad (1)$$

where  $\mathbf{z}_i = \mathcal{F}(\mathbf{x}_i)$  is the 2D Discrete Fourier Transform of  $\mathbf{x}_i$ .  $\theta(\cdot; r)$  denotes a thresholding function that separates the different frequency components from  $\mathbf{z}_i$  according to the radii  $r_1, \dots, r_N$ . Formally, for an one-channel image  $x \in \mathcal{N}$  where  $\mathcal{N}$  possible pixel values. Then, we obtain  $\mathbf{z} \in \mathbb{C}^{m \times n}$ , where  $\mathbb{C}$  denotes the set of complex numbers. The value of  $\mathbf{z}$  at coordinates  $(x, y)$  is denoted by  $\mathbf{z}(x, y)$ , while  $(c, c')$  represents the centroid. The formal definition of  $\mathbf{z}_i$  is given

as:

$$\mathbf{z}_i = \{\mathbf{z}(x, y) \mid r_{i-1} \leq d((x, y), (c, c')) \leq r_i\},$$

we consider  $d(\cdot, \cdot)$  as the Euclidean distance, which operates independently on every channel of pixels.

All experiments in this section utilize ResNet18 [11] as the backbone, implemented in PyTorch [21]. Modifications to the network blocks are depicted in Fig. 2. The network is trained on the CIFAR-10 dataset using CrossEntropyLoss, with the SGD optimizer set to a learning rate of 0.1. We evaluate the classification performance on different frequency components of the input images at each training epoch. Changes in accuracy over time provide insights into the learning dynamics within the frequency domain [31]. To avoid the occasionality, we calculated the average over three training runs.

#### 3.1. Effect of Element-wise Product

Inspired by the *convolution theorem*, we first give a theoretical insight of why element-wise product can encourage NNs to learn on various frequency components from a frequency view.

**Theorem 1 (Convolution Theorem).** Consider two functions  $u(x)$  and  $v(x)$  with their Fourier transforms  $U$  and  $V$ :

$$(u \cdot v)(x) = \mathcal{F}^{-1}(U * V),$$

where  $\cdot$  and  $*$  means the element-wise product and convolution respectively.  $\mathcal{F}$  refers to the Fourier transform operator where  $\mathcal{F}[f(t)] = F(\omega) = \int_{-\infty}^{+\infty} f(t)e^{-j\omega t} dt$ . The convolution theorem indicates that the element-wise multiplication in the spatial domain equals to the convolution operation in the frequency domain. Let's consider the simplest situation which is the self-convolution of a function. Denoting the support set of  $\mathcal{F}(\omega)$  is  $[-\Omega, \Omega]$ , the support set of  $\mathcal{F} * \mathcal{F}(\omega)$  will be  $[-2\Omega, 2\Omega]$ . It means that self-convolution resulting in a broader frequency spectrum. With richer frequency information, NNs have more chances to learn both high-frequency and low-frequency components.

To verify this insight, we conduct experiments on the Res18 and Res18-Ewp to find the effect of element-wise product. As shown in Fig. 3a, the accuracy curve of Res18-Ewp visibly surpass that of Res18 for decomposed parts in ranges of  $(0, r_1)$  and early epochs in ranges of  $(r_1, r_2)$ . The results demonstrate that broader spectral ranges enable the network to learn faster and better across multiple frequency components. Empirically, it is usually the lower-frequency components. However, examining the accuracy curve for components within the range  $(r_2, r_3)$  reveals a significant drop in accuracy growth after 40 epochs compared to the base model. It indicates that although element-wise product can encourage the model learn faster on some frequency components, newly introduced high-frequencies can become the noise to disturb the effective learning on

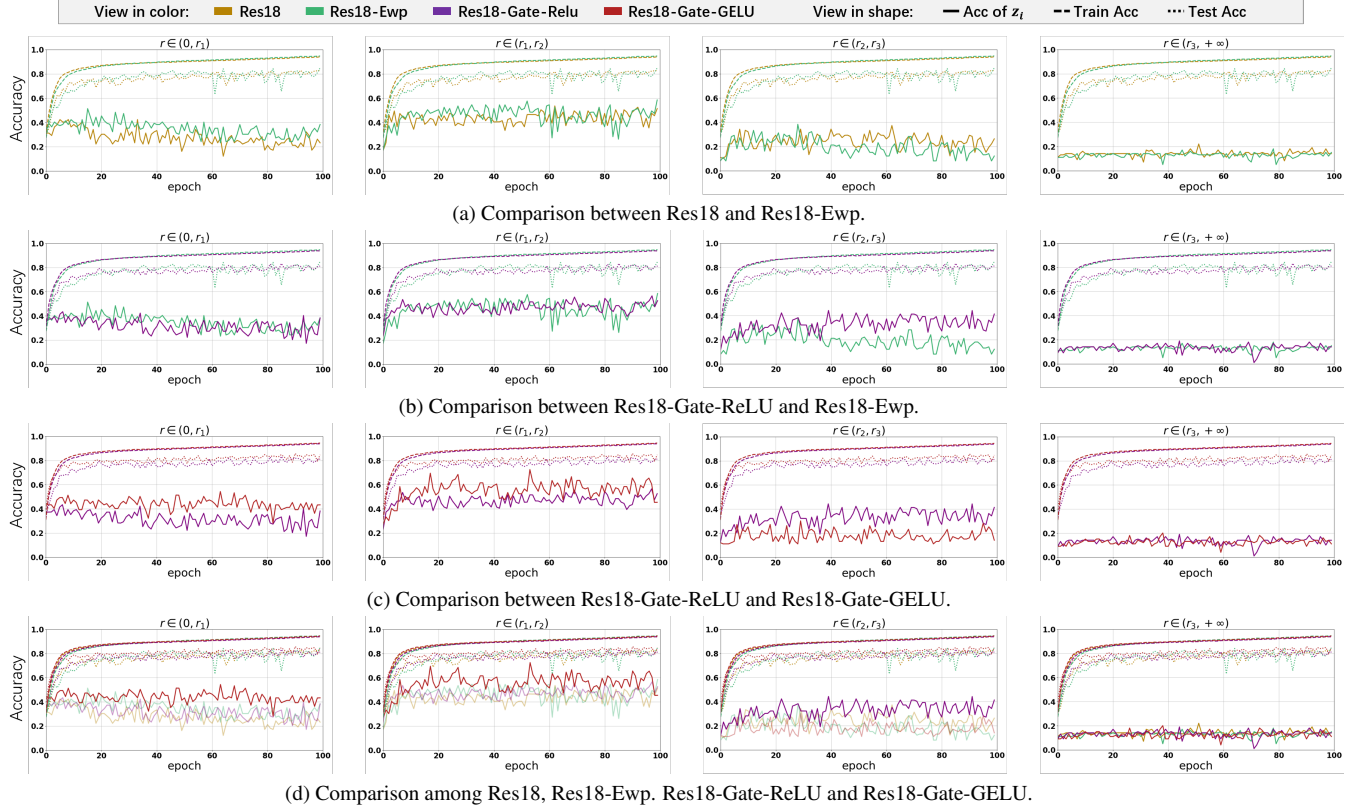


Figure 3. Learning curves of Resnet18 and its variants for 100 epochs, together plotted with the accuracy of different frequency components  $\mathbf{z}_i$ . We set  $\{r_1, r_2, r_3\}$  to  $\{6, 12, 18\}$ . All curves of  $\mathbf{z}_i$  are from the test set. The legends can be found in the top of Fig. 3(a). All the variants shows almost same training curves and very close testing curves of the raw data where the difference is lower than 0.03 on average. In this case, a difference value of 0.1 can be seen as a significant change. When accuracy falls below 15%, it can be considered close to the random selection, suggesting that neural networks struggle to learn from this particular frequency range. For a better view, we only put curves of two variants in a single image for figures a, b and c. Also, we plot all curves in a single plot and highlighted the most upper curves for each images in (d) to have a comprehensive understanding. More results on other settings can be found in the supplementary.

high-frequencies. Therefore, the activation layer is necessary to regulate the newly generated frequencies, minimizing the impact of high-frequency noise.

### 3.2. How Activation Function Works?

In this paper, we mainly focus on two kinds of activation functions based on their properties.

- Smooth activation: Smooth function means the differential coefficient is continuous like GELU and Swish. This type of functions usually tends to produce lower frequency components.
- Non-smooth activation: Functions like ReLU and ReLU6 have discontinuous derivatives, which can introduce more high-frequency components in gating mechanisms.

Specially, we select GELU and ReLU as representations to reveal how two kinds of activation functions control the new generated frequencies differently.

#### 3.2.1. Theoretical Demonstrations

We firstly give a brief mathematical analysis of how the differential properties of activating functions affect the frequency extension in GLUs.

**Theorem 2** (Differential Properties of the Fourier Transform). *If a function  $f(t)$  is continuous in  $(-\infty, +\infty)$ , then*

$$\mathcal{F}[f'(t)] = j\omega F[\omega]$$

*Proof.*

$$\begin{aligned} \mathcal{F}[f'(t)] &= \int_{-\infty}^{+\infty} f'(t)e^{-j\omega t} dt \\ &= f(t)e^{-j\omega t} \Big|_{-\infty}^{+\infty} + j\omega \int_{-\infty}^{+\infty} f(t)e^{-j\omega t} dt \\ &= j\omega \mathcal{F}[f(t)] \end{aligned}$$

□

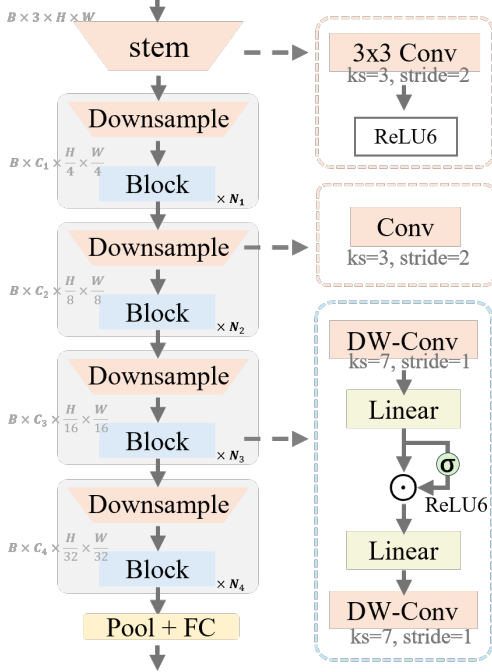


Figure 4. The illustration of GmNet architecture. GmNet adopts a traditional hybrid architecture, utilizing convolutional layers to down-sample the resolution and double the number of channels at each stage. Several blocks are repeated to extract features.

The definitions of the symbols are same to Theorem 1.

**Lemma 3.** If  $f^{(n)}(t)$  is continuous in  $(-\infty, +\infty)$ , then

$$\mathcal{F}[f^{(n)}(t)] = (j\omega)^n F[\omega], \quad (2)$$

where  $f^{(n)}(t)$  represents the  $n$ -th derivative of  $f(t)$ . The proof of Lemma 2 can be easily obtained by the mathematical induction based on Theorem 2. From Eq. 2, we can find that  $|F(\omega)| \leq \frac{C}{|\omega|^n}$  where  $C$  is a sufficiently large constant. It indicates that if higher-order derivatives exist and are continuous, the high-frequency components of the Fourier transform decay more quickly with a rate of  $|\omega|^n$ . Conversely, if higher-order derivatives do not exist or are discontinuous, the decay of the high-frequency components of the Fourier transform slows down. Notably, for the smooth activation like  $\text{GELU}(x) = x \cdot \frac{1}{2}[1 + \text{erf}(x/\sqrt{2})]$ , it is infinitely differentiable across the entire real domain, with all orders of derivatives being continuous and finite. The continuity and finite values of higher-order derivatives cause the high-frequency components of the Fourier transform to decay quickly, resulting in fewer high-frequency components. On the other hand, discontinuity of higher-order derivatives can lead to generating more high-frequencies. Non-smooth activation may encourage remaining more higher frequency components in the gating mechanism.

Table 1. Configurations of GmNet. We vary the embed width, the depth and the ratio to build different sizes of GmNet.

Variant	$C_1$	depth	ratio	Params	FLOPs
GmNet-S1	40	[2, 2, 10, 2]	[3, 3, 3, 2]	3.7M	0.6G
GmNet-S2	48	[2, 2, 8, 3]	[3, 3, 3, 2]	6.2M	0.9G
GmNet-S3	48	[3, 3, 8, 3]	[4, 4, 4, 4]	7.8M	1.2G
GmNet-S4	68	[3, 3, 11, 3]	[4, 4, 4, 4]	17.0M	2.7G

### 3.2.2. Experimental Analysis

As shown in Fig. 3b, compared to the model without activation, the complete gating unit (using ReLU) learns better in higher frequency components compared to Res18-Ewp, like in  $\mathbf{z}_i \in (r_2, r_3)$ . It effectively avoids the disturbance of high-frequency noise. Moreover, we have conducted contrast experiments of using different kinds of activation functions. From Fig. 3c, it is obvious that the model using non-smooth activation (ReLU) performs better in learning from the higher-frequencies like  $(r_2, r_3)$ . The superiority of the variant with GELU when  $r \in (0, r_2)$  shows the capability of the smooth activation function in learning lower-frequency components. Also, the performance of Res18-Gate-GELU on  $(r_2, r_3)$  which is under 20% also indicates the low-frequency bias for the smooth activation function. Additionally, as shown in Fig. 3d, GELU and ReLU demonstrate their superiority among the variants in capturing low-frequency and high-frequency components, respectively. It indicates that the model with a complete gating unit can better capture the information for various ranges of frequency based on their properties.

**Discussions.** Different datasets and training strategies may lead to different dynamics which has been addressed in [26, 31]. For the small dataset, the convergence is faster which means NNs can easily capture some certain frequency components and then learning from other frequency components becomes very slow. Therefore, the generated high-frequency noise has a greater impact on disturbing the learning from high-frequencies. We will show more evidences and discussions of the difference between various activation functions in ablation studies on a larger dataset. Moreover, from the performance on very high-frequency components (for  $\mathbf{z}_i \in (r_3, +\infty)$ ), it is evident that neural networks face challenges in directly classifying these components, which are nearly imperceptible to the human eye. However, NNs can be sensitive to the perturbation of high-frequency noise [34]. This is also an interesting topic of revealing the robustness of NNs, but it is beyond the scope of this article.

## 4. Method

To address the limitation of low-frequency bias for CNN-based network designs, our proposed method named as GmNet integrates a simple gated linear unit into the block as il-

Table 2. Comparison of Efficient Models on ImageNet-1k. Latency is evaluated across various platforms, including A100 GPU and iPhone 14 mobile device. Latency benchmarking batch size is set to 1 as in real-world scenario.

Model	Top-1		FLOPs (G)	Latency (ms)	
	Params (%)	(M)		GPU	Mobile
MobileV2-1.0 [23]	72.0	3.4	0.3	1.7	0.9
ShuffleV2-1.5 [17]	72.6	3.5	0.3	2.2	1.3
EfficientFormerV2-S0 [15]	73.7	3.5	0.4	2.0	0.9
StarNet-S2 [18]	74.8	3.7	0.5	1.9	0.9
<b>GmNet-S1</b>	<b>75.5</b>	3.7	0.6	<b>1.6</b>	1.0
FasterNet-T0 [2]	71.9	3.9	0.3	2.5	0.7
EfficientFormerV2-S1 [15]	77.9	4.5	0.7	3.4	1.1
EfficientMod-xxs [19]	76.0	4.7	0.6	2.3	18.2
RepViT-M0.9 [30]	77.4	5.1	0.8	3.0	1.1
StarNet-S3 [18]	77.3	5.8	0.7	2.3	1.1
<b>GmNet-S2</b>	<b>78.3</b>	6.2	0.9	<b>1.9</b>	1.1
EfficientMod-xs [19]	78.3	6.6	0.8	2.9	22.7
EdgeViT-XS [20]	77.5	6.8	1.2	3.0	1.6
RepViT-M1.0 [30]	78.6	6.8	1.2	3.6	1.1
StarNet-S4 [18]	78.4	7.5	1.1	3.3	1.1
Fasternet-T1 [2]	76.2	7.6	0.9	2.5	1.0
MobileOne-S2 [28]	77.4	7.8	1.3	1.8	1.0
<b>GmNet-S3</b>	<b>79.3</b>	7.8	1.2	2.1	1.3
RepViT-M1.1 [30]	79.4	8.3	1.3	5.1	1.2
FastViT-S12 [27]	79.8	8.8	1.8	5.3	1.6
EfficientFormer-L1 [14]	77.2	12.3	1.3	12.1	1.4
EfficientFormerV2-S2 [15]	80.4	12.7	1.3	5.4	1.6
EfficientMod-s [19]	81.0	12.9	1.4	4.5	35.3
RepViT-M1.5 [30]	81.2	14.0	2.3	6.4	1.7
MobileOne-S4 [28]	79.4	14.8	2.9	2.9	1.8
LeViT-256 [8]	81.5	18.9	1.1	6.7	31.4
<b>GmNet-S4</b>	<b>81.5</b>	17.0	2.7	<b>2.9</b>	1.9

illustrated in Fig. 4. GmNet offers both theoretical and practical advantages on encouraging the model to learn from a broader range of frequency regions, especially the high-frequency domain. We incorporate two depth-wise convolution layers with kernel sizes of  $7 \times 7$  at the beginning and end of the block respectively to facilitate the integration of low- and high-frequency information. At the core of the block, we have two  $1 \times 1$  convolution layers and a simple gated linear unit. We use the ReLU6 as the activation function. ReLU6 can not only emphasize the higher frequency components since it has discontinuous higher derivatives, but also it can limit the amplitudes and energy of the high-frequency components with limiting the max values. We vary the block numbers, input embedding channel numbers and channel expansion factors ‘ratio’ to build different sizes of GmNet, as detailed in Table 1.

GmNet uses a simplified GLU structure for two reasons: (1) to keep the model as lightweight as possible, reducing computational load; and (2) ensuring that high-frequency signals can be better enhanced without adding any additional convolutional or fully connected layers within the

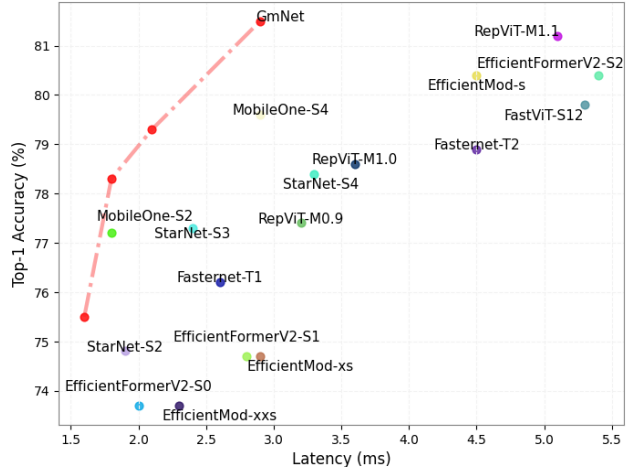


Figure 5. Trade-off between Top-1 accuracy and latency on A100. GmNet variants achieve substantially lower latency compared to related works. A more extensive comparison is provided in the supplementary material.

GLU. Furthermore, our gate unit is more interpretable, aligning with our analysis of GLUs in the frequency domain. Experimental results and ablation studies consistently demonstrate the superiority of our model, validating its design in accordance with our GLU frequency domain studies. We also show that the simplest structure achieves the optimal trade-off between efficiency and effectiveness.

## 5. Experiments

In this section, we provide extensive experiments to show the superiority of our model and ample ablation studies to demonstrate the effectiveness of components of our method.

### 5.1. Results in Image Classification

**Implementation details.** We perform image classification experiments on the ImageNet-1K dataset, adopting a standard input resolution of  $224 \times 224$  for both training and evaluation. All model variants are trained from scratch for 300 epochs using the AdamW optimizer, starting with an initial learning rate of  $3 \times 10^{-3}$  and a batch size of 2048. The supplementary materials provide a comprehensive overview of the training setup. For performance assessment, we convert our PyTorch models into the ONNX format to measure latency on a Mobile device (iPhone 14) and a GPU (A100). Additionally, we deploy the models on the mobile device via CoreML-Tools to further evaluate latency. Importantly, our training approach does not incorporate advanced techniques such as re-parameterization or knowledge distillation. The results presented in Table 2 correspond to models trained without these enhancements.

**Compared with the state-of-the-art.** The experimental results are presented in Table 2. Without any strong training

Activation	Identity		ReLU		GELU		ReLU6	
Raw data	70.5		78.3		78.4		79.3	
Frequency	Low	High	Low	High	Low	High	Low	High
$r = 12$	9.79	12.6	12.0	45.9	12.7	41.5	14.8	51.7
$r = 24$	38.1	1.7	38.6	13.5	40.0	9.4	41.6	12.1
$r = 36$	52.9	0.7	56.2	4.9	58.7	3.9	55.2	4.7
$r = 48$	63.2	0.5	64.5	2.3	66.1	2.1	64.4	2.5
$r = 60$	66.6	0.9	69.4	1.0	70.7	1.1	71.1	1.4

Table 3. The accuracies of classifying the raw data and their low-/high-frequency components under different activation functions on ImageNet-1k. We gradually increase the radii by a step of 12. This result is the average of five testings.

strategy, GmNet delivers impressive performance compared to many state-of-the-art lightweight models. With a comparable latency on GPU, GmNet-S1 outperforms MobileV2-1.0 by 3.5%. Notably, GmNet-S2 achieves 78.3% with only 1.9ms on the A100 which is a remarkable achievements for the models under 1G FLOPS. GmNet-S3 outperforms RepViT-M1.0 and StarNet-S4 by 1.9% and 0.9% in top-1 accuracy with 1.1 ms and 1.4 ms faster on the GPU latency, respectively. The improvements on the speed are over 30%. Additionally, with similar latency, GmNet-S3 delivers a 1.7% improvement on the accuracy over MobileOne-S4. GmNet-S4 achieves 2x faster compared to RepViT-M1.5 on the GPU and it surpasses MobileOne-S4 of 2.1% under the similar latencies of both GPU and Mobile. LeViT-256 [8] matches the accuracy of GmNet-S4 but runs twice as slow on a GPU and 16 times slower on an iPhone 14. The strong performance of GmNet can be largely attributed to the clear insights of gating mechanisms and simplest architectures. Fig. 5 further illustrates the latency-accuracy trade-off across different models. More comparisons and results of downstream tasks including objective detection and segmentation can be found in supplementary.

## 5.2. Ablation Studies

**More studies on different activation functions.** To further explore the effect of different activation functions, we trained various GmNet-S3 variants on ImageNet-1k. As illustrated in Fig. 4, we replaced ReLU6 with GELU, ReLU or remove the activation function. To better reflect the differences between different models, we set the radii to a larger range and only separate the decomposed image into two kinds of frequency components. For  $\mathbf{z}_i \in (0, r)$ , we recognize it as the low-frequency component while  $\mathbf{z}_i \in (r, +\infty)$  represents the high-frequency component [31, 32]. As shown in the Table. 3, we can find that, the increases on classifying the high-frequency components are significant comparing models using and not using the activation functions. For example, comparing results of ‘Identity’ and ‘ReLU’ with the improvement of 11% on the raw data, improvement on high-frequencies is over 3 times on average. ‘GELU’ and ‘ReLU’ shows advances on low-/high- frequency components respectively compared to each

Methods	Top-1 (%)	$r = 12$		$r = 24$		$r = 36$	
		High	Low	High	Low	High	Low
MobileOne-S2 [28]	77.4	35.0	11.6	6.5	36.9	2.4	53.5
EfficientMod-xs [19]	78.3	45.4	12.9	9.4	40.6	3.5	54.6
StarNet-S4 [18]	78.4	43.3	13.8	9.4	41.3	3.4	54.8
GmNet-S3	<b>79.3</b>	<b>51.7</b>	<b>14.8</b>	<b>12.1</b>	<b>41.6</b>	<b>4.7</b>	<b>55.2</b>

Table 4. Comparison with recent methods. We test the models on the high-/low-frequency components with different radii on the ImageNet-1k. The highest values of each columns are highlighted.

other. This aligns with our understanding of how different types of activation functions impact frequency response. Notably, the closer performance of models with Identity and ReLU/GELU at low frequencies suggests the low-frequency bias of convolution-based networks.

Moreover, even considering the improvements on the raw data, model using the ReLU6 shows obvious increase on the high-frequency components compared to the model using GELU especially when we set  $r$  to 12, 24, 36. Compared to the model with ReLU, ReLU6 is more effective in preventing overfitting to high-frequency components since it has better performance on low-frequencies. Considering performances of ReLU, GELU, and ReLU6, we can observe that achieving better performance on high frequencies at the expense of lower frequencies does not necessarily lead to overall improvement, and vice versa. To get a better performance on the raw data, it is essential to enhance the model’s ability to learn various frequency signals without compromising others.

**Comparison with existing methods.** As addressed in Table 3, a model should achieves strong performance across different frequency components to deliver a better overall performance. However, both pure convolutional architectures and transformers exhibit a low-frequency bias, as discussed in [1, 26]. Therefore, enhancing the performance of a lightweight model depends on its ability to more effectively capture high-frequency information.

To address the advantages of GmNet on overcoming the low-frequency bias, we test some existing models on different frequency components of different radii. We select three kinds of typical lightweight methods for comparison including pure conv-based model MobileOne-S2 [28], attention-based model EfficientMod-xs [19] and model also employing GLUs-like structure StarNet-S4 [18]. As shown in Table 4, accuracies of low-frequency components are close among different models considering the overall performance. However, it shows that GmNet-S3 clearly surpass the other models in high frequency components. For example, GmNet-S3 has a 6.3% improvement compared to EfficientMod-xs when  $r = 12$  and 2.7% increase when  $r = 24$ . For StarNet, which also uses a GLU-like structure with dual-channel FC, it struggles to effectively

Table 5. Comparison of different GLU designs for GmNet-S3 on ImageNet-1K. Here, LN, DW, and Pool represent layer normalization, depth-wise convolution with a kernel size of 3, and average pooling with a 3×3 window, respectively. We underline all notable scores in classifying the different frequency decompositions. Considering gaps of overall performances, an improvement which is remarkable should exceed 1.0. This result is the average of five testings. We also provide more variants of GLUs in the supplementary materials.

GLUs	Top-1 (%)	Params (M)	GPU (ms)	$r = 12$		$r = 24$		$r = 36$		$r = 48$		$r = 60$	
				Low	High	Low	High	Low	High	Low	High	Low	High
$\sigma(x) \cdot \text{LN}(x)$	78.9	7.8	2.9	12.1	47.6	41.6	10.9	56.4	<u>5.2</u>	64.7	2.4	69.8	1.2
$\sigma(x) \cdot \text{DW}(x)$	79.0	8.0	2.4	12.3	49.0	<u>42.7</u>	9.6	58.1	<u>4.6</u>	65.7	2.3	71.2	1.1
$\sigma(x) \cdot (x - \text{Pool}(x))$	78.6	7.8	2.4	14.2	50.1	<u>42.3</u>	10.8	<u>55.8</u>	4.9	<u>63.8</u>	2.7	<u>69.9</u>	1.3
$\sigma(x) \cdot x$	79.3	7.8	2.1	<u>14.8</u>	<u>51.7</u>	41.6	<u>12.1</u>	55.2	4.7	64.4	2.5	71.1	1.4

emphasize high-frequency signals. The simplest GLUs design can deliver a better learning on various frequency components and it can achieve a better balance between the efficiency and the effectiveness.

**Study on designs of the GLU.** In GmNet, the gated linear unit adopts the simplest design, which can be defined as  $\sigma(x) \cdot x$ . For comparison, we modify the GLU design and conduct experiments to test performance on raw data as well as on decompositions at different frequency levels. As shown in the Table 5, the simplest design achieve the best performance both on effectiveness and efficiency for the overall performance. For the decomposed frequency components, we observe clear differences among various GLU designs. The GLU of  $\sigma(x) \cdot x$  demonstrates significantly higher accuracy in classifying high-frequency components. For example, for  $r = 12$  and  $r = 24$ , the GLU with  $\sigma(x) \cdot x$  shows an improvement of 4.1 over the LN design and 2.5 over the DW design. This indicates that the simplest GLU design is already effective at introducing reliable high-frequency components to enhance the model’s ability to learn them. Designs aimed at smoothing information show a notable improvement in some low-frequency components. For instance, with similar overall performance, the GLUs using  $\sigma(x) \cdot \text{DW}(x)$  and  $\sigma(x) \cdot \text{LN}(x)$  achieve better results on low-frequency components when the radii are set to 24, 36, and 48. And depth-wise convolution is more effective than layer normalization in encouraging neural networks to learn from low-frequency components which is also more efficient. For the design with the average pooling, it does not perform better in classifying high-frequency signals. This may be because  $x - \text{pool}(x)$  acts as an overly aggressive high-pass filter, which does not retain the original high-frequency signals in  $x$  well and instead introduces more high-frequency noise.

**Bandwidths analysis of convolution kernels.** As discussed in the [26], the convolution layer may play roles of ‘smoothing’ the feature which means it has a low-frequency bias. Experiments on studying weights of the convolution layer is insightful to give more evidences of how GLUs effect the learning of different frequency components [1, 26, 31]. In this paper, we propose using

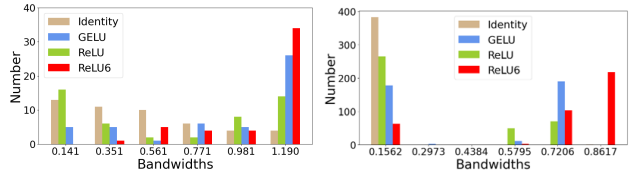


Figure 6. The histogram illustrates the distribution of bandwidths of convolution kernels. We use weights of the convolution layer which under the GLU in the first block (left) and the last block (right) of the GmNet-S3. All modals are trained on the raw data of the ImageNet-1k. In general, the further the distribution shifts to the right, the stronger the convolutional kernel’s ability to capture signals of different frequencies.

the bandwidths of convolution kernels to represent their ability of responding to different frequency components. Specifically, a wider bandwidth indicates that the kernel can process a broader range of frequencies, allowing it to capture diverse frequency components simultaneously and thereby preserve rich information from the feature. As illustrated in Figure 6, the distributions of the ReLU model suggest that its convolution kernels tend to focus on a narrow range of frequency components leading to relatively lower bandwidths. It indirectly reflects an overemphasis on high-frequency components. Although the model using GELU exhibits a better distribution in the top convolutional layers, it still has a low-frequency bias, leading to a distribution shift in the bottom convolutional layers. Compared to other activations, the enhanced bandwidth distribution of the model using ReLU6 demonstrates better generalization for this task. The properties of the convolution kernels align with the results in Table 3.

## 6. Conclusion

In this paper, we systematically explore the effect of gating mechanisms on the training dynamics of neural networks from a frequency perspective. We provide both theoretical and experimental analysis to reveal how the element-wise product and activation interplay to manage the balance between different frequencies learning. The element-wise product can broaden the spectrum of the signals while introduce high-frequency noise. The activation function

can effectively control the frequency output based on its own characters. Benefited by the comprehensive study on GLUs, we introduce a lightweight model named GmNet to efficiently utilize the information of various frequency. It shows impressive performance on both effectiveness and efficiency compared with recent lightweight models.

## References

- [1] Jiawang Bai, Li Yuan, Shu-Tao Xia, Shuicheng Yan, Zhifeng Li, and Wei Liu. Improving vision transformers by revisiting high-frequency components. In *European Conference on Computer Vision*, pages 1–18. Springer, 2022. 3, 7, 8
- [2] Jierun Chen, Shiu-hong Kao, Hao He, Weipeng Zhuo, Song Wen, Chul-Ho Lee, and S-H Gary Chan. Run, don’t walk: chasing higher flops for faster neural networks. In *Proceedings of the IEEE/CVF conference on computer vision and pattern recognition*, pages 12021–12031, 2023. 6
- [3] Junyoung Chung, Caglar Gulcehre, KyungHyun Cho, and Yoshua Bengio. Empirical evaluation of gated recurrent neural networks on sequence modeling. *arXiv preprint arXiv:1412.3555*, 2014. 1
- [4] Yann N Dauphin, Angela Fan, Michael Auli, and David Grangier. Language modeling with gated convolutional networks. In *International conference on machine learning*, pages 933–941. PMLR, 2017. 1, 2
- [5] Soham De, Samuel L Smith, Anushan Fernando, Aleksandar Botev, George Cristian-Muraru, Albert Gu, Ruba Haroun, Leonard Berrada, Yutian Chen, Srivatsan Srinivasan, et al. Griffin: Mixing gated linear recurrences with local attention for efficient language models. *arXiv preprint arXiv:2402.19427*, 2024. 1
- [6] Abhimanyu Dubey, Abhinav Jauhri, Abhinav Pandey, Abhishek Kadian, Ahmad Al-Dahle, Aiesha Letman, Akhil Mathur, Alan Schelten, Amy Yang, Angela Fan, et al. The llama 3 herd of models. *arXiv preprint arXiv:2407.21783*, 2024. 1, 2
- [7] Felix A Gers, Jürgen Schmidhuber, and Fred Cummins. Learning to forget: Continual prediction with lstm. *Neural computation*, 12(10):2451–2471, 2000. 2
- [8] Benjamin Graham, Alaaeldin El-Nouby, Hugo Touvron, Pierre Stock, Armand Joulin, Hervé Jégou, and Matthijs Douze. Levit: a vision transformer in convnet’s clothing for faster inference. In *Proceedings of the IEEE/CVF international conference on computer vision*, pages 12259–12269, 2021. 6, 7
- [9] Alex Graves and Jürgen Schmidhuber. Framewise phoneme classification with bidirectional lstm and other neural network architectures. *Neural networks*, 18(5-6):602–610, 2005. 2
- [10] Albert Gu and Tri Dao. Mamba: Linear-time sequence modeling with selective state spaces. *arXiv preprint arXiv:2312.00752*, 2023. 1, 2
- [11] Kaiming He, Xiangyu Zhang, Shaoqing Ren, and Jian Sun. Deep residual learning for image recognition. In *Proceedings of the IEEE conference on computer vision and pattern recognition*, pages 770–778, 2016. 3
- [12] Dan Hendrycks and Kevin Gimpel. Gaussian error linear units (gelus). *arXiv preprint arXiv:1606.08415*, 2016. 2
- [13] S Hochreiter. Long short-term memory. *Neural Computation MIT-Press*, 1997. 1, 2
- [14] Yanyu Li, Geng Yuan, Yang Wen, Ju Hu, Georgios Evangelidis, Sergey Tulyakov, Yanzhi Wang, and Jian Ren. Efficientformer: Vision transformers at mobilenet speed. *Advances in Neural Information Processing Systems*, 35: 12934–12949, 2022. 2, 6
- [15] Yanyu Li, Ju Hu, Yang Wen, Georgios Evangelidis, Kamyar Salahi, Yanzhi Wang, Sergey Tulyakov, and Jian Ren. Re-thinking vision transformers for mobilenet size and speed. In *Proceedings of the IEEE/CVF International Conference on Computer Vision*, pages 16889–16900, 2023. 6
- [16] Hanxiao Liu, Zihang Dai, David So, and Quoc V Le. Pay attention to mlps. *Advances in neural information processing systems*, 34:9204–9215, 2021. 1, 2
- [17] Ningning Ma, Xiangyu Zhang, Hai-Tao Zheng, and Jian Sun. ShuffleNet v2: Practical guidelines for efficient cnn architecture design. In *Proceedings of the European conference on computer vision (ECCV)*, pages 116–131, 2018. 6
- [18] Xu Ma, Xiyang Dai, Yue Bai, Yizhou Wang, and Yun Fu. Rewrite the stars. In *Proceedings of the IEEE/CVF Conference on Computer Vision and Pattern Recognition*, pages 5694–5703, 2024. 1, 2, 6, 7
- [19] Xu Ma, Xiyang Dai, Jianwei Yang, Bin Xiao, Yinpeng Chen, Yun Fu, and Lu Yuan. Efficient modulation for vision networks. *arXiv preprint arXiv:2403.19963*, 2024. 2, 6, 7
- [20] Junting Pan, Adrian Bulat, Fuwen Tan, Xiatian Zhu, Lukasz Dudziak, Hongsheng Li, Georgios Tzimiropoulos, and Brais Martinez. Edgevits: Competing light-weight cnns on mobile devices with vision transformers. In *European Conference on Computer Vision*, pages 294–311. Springer, 2022. 6
- [21] Adam Paszke, Sam Gross, Francisco Massa, Adam Lerer, James Bradbury, Gregory Chanan, Trevor Killeen, Zeming Lin, Natalia Gimelshein, Luca Antiga, et al. Pytorch: An imperative style, high-performance deep learning library. *Advances in neural information processing systems*, 32, 2019. 3
- [22] Nasim Rahaman, Aristide Baratin, Devansh Arpit, Felix Draxler, Min Lin, Fred Hamprecht, Yoshua Bengio, and Aaron Courville. On the spectral bias of neural networks. In *International conference on machine learning*, pages 5301–5310. PMLR, 2019. 2
- [23] Mark Sandler, Andrew Howard, Menglong Zhu, Andrey Zhmoginov, and Liang-Chieh Chen. Mobilenetv2: Inverted residuals and linear bottlenecks. In *Proceedings of the IEEE conference on computer vision and pattern recognition*, pages 4510–4520, 2018. 6
- [24] Noam Shazeer. Glu variants improve transformer. *arXiv preprint arXiv:2002.05202*, 2020. 2
- [25] Matthew Tancik, Pratul Srinivasan, Ben Mildenhall, Sara Fridovich-Keil, Nithin Raghavan, Utkarsh Singhal, Ravi Ramamoorthi, Jonathan Barron, and Ren Ng. Fourier features let networks learn high frequency functions in low dimensional domains. *Advances in neural information processing systems*, 33:7537–7547, 2020. 2

- [26] Ling Tang, Wen Shen, Zhanpeng Zhou, Yuefeng Chen, and Quanshi Zhang. Defects of convolutional decoder networks in frequency representation. *arXiv preprint arXiv:2210.09020*, 2022. [3](#), [5](#), [7](#), [8](#)
- [27] Pavan Kumar Anasosalu Vasu, James Gabriel, Jeff Zhu, Oncel Tuzel, and Anurag Ranjan. Fastvit: A fast hybrid vision transformer using structural reparameterization. In *Proceedings of the IEEE/CVF International Conference on Computer Vision*, pages 5785–5795, 2023. [6](#)
- [28] Pavan Kumar Anasosalu Vasu, James Gabriel, Jeff Zhu, Oncel Tuzel, and Anurag Ranjan. Mobileone: An improved one millisecond mobile backbone. In *Proceedings of the IEEE/CVF conference on computer vision and pattern recognition*, pages 7907–7917, 2023. [2](#), [6](#), [7](#)
- [29] A Vaswani. Attention is all you need. *Advances in Neural Information Processing Systems*, 2017. [1](#)
- [30] Ao Wang, Hui Chen, Zijia Lin, Jungong Han, and Guiguang Ding. Reprivit: Revisiting mobile cnn from vit perspective. In *Proceedings of the IEEE/CVF Conference on Computer Vision and Pattern Recognition*, pages 15909–15920, 2024. [2](#), [6](#)
- [31] Haohan Wang, Xindi Wu, Zeyi Huang, and Eric P Xing. High-frequency component helps explain the generalization of convolutional neural networks. In *Proceedings of the IEEE/CVF conference on computer vision and pattern recognition*, pages 8684–8694, 2020. [2](#), [3](#), [5](#), [7](#), [8](#)
- [32] Zhi-Qin John Xu, Yaoyu Zhang, Tao Luo, Yanyang Xiao, and Zheng Ma. Frequency principle: Fourier analysis sheds light on deep neural networks. *arXiv preprint arXiv:1901.06523*, 2019. [7](#)
- [33] Jianwei Yang, Chunyuan Li, Xiyang Dai, and Jianfeng Gao. Focal modulation networks. *Advances in Neural Information Processing Systems*, 35:4203–4217, 2022. [1](#)
- [34] Dong Yin, Raphael Gontijo Lopes, Jon Shlens, Ekin Dogus Cubuk, and Justin Gilmer. A fourier perspective on model robustness in computer vision. *Advances in Neural Information Processing Systems*, 32, 2019. [2](#), [5](#)